Journal of the Optical Society of America B
OPTICAL PHYSICS

Spatial beam narrowing in Raman amplifiers made with graded-index multimode fibers: a semi-analytic approach

GOVIND P. AGRAWAL
The Institute of Optics, University of Rochester, Rochester, New York 14627, USA (gpa@optics.rochester.edu)

Received 2 December 2022; revised 13 February 2023; accepted 14 February 2023; posted 14 February 2023; published 8 March 2023

A semi-analytic model of the amplification process is presented for Raman amplifiers made with graded-index multimode fibers. When the pump beam remains much more intense than the signal being amplified, it evolves in a self-similar fashion and recovers its initial width periodically. Using this feature, the width of the amplified signal is found to satisfy an equation whose form is similar to that of a damped harmonic oscillator. We use this equation to discuss the spatial beam narrowing occurring inside a Raman amplifier. In addition to oscillating with a period ∼1 mm, the beam also narrows down during its amplification inside a graded-index fiber on a length scale ∼1 m. The main advantage of our simplified approach is that it provides an analytic expression for the damping distance of width oscillations that shows clearly the role played by various physical parameters.

https://doi.org/10.1364/JOSAB.482730

1. INTRODUCTION

Step-index silica fibers have been used for making Raman amplifiers for nearly 50 years, and such amplifiers are used for a variety of applications [1–3]. In recent years, graded-index (GRIN) multimode fibers have been used as Raman amplifiers, mainly motivated by two properties of such fibers. First, a larger core diameter allows for higher output powers exceeding kilowatt levels [4–7]. Second, the spatial quality of the amplified beam is improved through a phenomenon known as the Raman-induced beam cleanup [8,9]. Self-imaging, an intrinsic property of GRIN fibers designed with a parabolic refractive-index profile [10], also plays an important role during the amplification process.

A mode-based description of the Raman-induced beam-cleanup process has shown that the use of GRIN fibers is essential for the improvement in the beam's quality [8]. It makes use of the modal overlap factors and reveals that the effective Raman gain is larger for lower-order Stokes modes. As a result, even when the incoming signal beam excites many modes of the GRIN fiber at the input end, most of its power appears in a few low-order modes of the fiber at the output end. An extensive numerical model of the Raman amplification process based on the modal expansion has been developed recently for studying brightness enhancement in GRIN-fiber Raman lasers [11]. It included important processes such as intracavity spatial filtering and random linear mode coupling, together with the nonlinear effects such as self-phase modulations (SPMs) and cross-phase modulations (XPMs). The predicted narrowing of the amplified beam agreed with the experimental data. By necessity, such a numerical model becomes time-consuming as more and more modes are taken into account. It also hinders physical insight and does not reveal what parameters are most relevant for beam narrowing to occur.

In this work, a semi-analytic model of the amplification process is developed for GRIN-fiber Raman amplifiers. Section 2 provides mathematical details and identifies the approximations that can be used to simplify the nonlinear coupled partial differential equations satisfying the pump and signal fields. An intense pump beam is found to evolve in a periodic fashion because of self-imaging. We use this solution in Section 3 to solve the equation governing amplification of the signal beam and show that its width satisfies an equation whose form is similar to that of a damped harmonic oscillator. This equation is employed in Section 4 to discuss spatial narrowing of the signal beam occurring during its amplification inside a GRIN-fiber Raman amplifier. The main results are summarized in Section 5.

2. THEORY OF GRIN-FIBER RAMAN AMPLIFIERS

We consider a GRIN fiber whose refractive index is designed to decrease radially in a parabolic fashion and can be written as

$$n(\rho) = n_0\left(1 - \frac{1}{2}b^2\rho^2\right) + n_2|E|^2, \tag{1}$$

where $\rho = \sqrt{x^2 + y^2}$ is the radial distance from the central axis of the GRIN fiber (aligned with the z axis) and n_0 is the refractive index at $\rho = 0$. The index gradient b is defined as $b = \sqrt{2\Delta}/a$, where a is the radius of the GRIN fiber's core and Δ is the relative core-cladding index difference. The nonlinear effects are included through the intensity dependence of the refractive index resulting from the optical Kerr effect. The Kerr coefficient n_2 has a value of about 2.7×10^{-20} m^2/W for silica fibers.

The pump and signal beams are launched at the input end of the GRIN fiber located at $z = 0$. The total electric field at a distance z can be written as

$$E(\mathbf{r}, t) = A_p \exp[i(k_p z - \omega_p t)] + A_s \exp[i(k_s z - \omega_s t)], \tag{2}$$

where $k_j = n_0(\omega_j)\omega_j/c$ with $j = p, s$ and $\Omega = \omega_p - \omega_s$ is the frequency shift of the signal from the pump (about 13.2 THz for maximum Raman gain). Both waves are assumed to remain polarized along the same direction.

For Raman amplification to occur, the nonlinear part, $n_2|E|^2$, of the refractive index is modified to include the Raman contribution as [2,12]

$$n_2|E|^2 = (1 - f_R)n_2|E|^2 + f_R n_2 \int_0^\infty h_R(t')|E(t - t')|^2 \mathrm{d}t', \tag{3}$$

where f_R is the fractional Raman contribution (about 18% for silica glass) and $h_R(t)$ is the Raman response function of the material used to make the GRIN device; it is normalized such that $\int_0^\infty h_R(t)\mathrm{d}t = 1$. Using Eq. (2) within the integral of Eq. (3), we obtain

$$\int_0^\infty h_R(t')|E(t - t')|^2 \mathrm{d}t' = |A_p|^2 + |A_s|^2 + A_p^* A_s e^{-i\delta k z}\tilde{h}_R(\Omega) + A_p A_s^* e^{i\delta k z}\tilde{h}_R^*(\Omega), \tag{4}$$

where $\delta k = k_p - k_s$ and $\tilde{h}_R(\Omega)$ is the Fourier transform of $h_R(t)$. The imaginary part of $\tilde{h}_R(\Omega)$ is related to the Raman gain [2] at the signal's frequency as $g_R = 2 f_R n_2(\omega_s/c)\mathrm{Im}(h_R)$.

When we use Eqs. (2)–(4) in Maxwell's equations, make the paraxial approximation, retain only the phase-matched terms, and separate the pump and signal terms, we obtain the following two coupled nonlinear equations for the pump and signal amplitudes [12]:

$$\frac{\partial A_p}{\partial z} + \frac{\nabla_T^2 A_p}{2ik_p} + \frac{i}{2}k_p b^2\rho^2 A_p = \frac{i\omega_p}{c}n_2(|A_p|^2 + 2|A_s|^2)A_p - \frac{\omega_p}{2\omega_s}g_R|A_s|^2 A_p - \alpha_p A_p, \tag{5}$$

$$\frac{\partial A_s}{\partial z} + \frac{\nabla_T^2 A_s}{2ik_s} + \frac{i}{2}k_s b^2\rho^2 A_s = \frac{i\omega_s}{c}n_2(|A_s|^2 + 2|A_p|^2)A_s + \frac{1}{2}g_R|A_p|^2 A_s - \alpha_s A_s, \tag{6}$$

where the loss of the GRIN fiber has been added through the last term. These equations include all linear and nonlinear effects for a GRIN Raman amplifier operating in a quasi-continuous fashion. In general, they must be solved numerically if one wants to include the diffractive and self-imaging effects together with the pump's depletion and resulting saturation of the Raman gain.

We are interested in finding an approximate solution of Eqs. (5) and (6), obtained with some reasonable assumptions. In practice, the pump beam is much more intense than the signal beam at the input end of the fiber. We make the assumption that the GRIN fiber is short enough that the pump is not depleted much and remains intense compared to the signal over the entire length of the Raman amplifier. If we also neglect losses over this length, Eqs. (5) and (6) are reduced to

$$\frac{\partial A_p}{\partial z} + \frac{\nabla_T^2 A_p}{2ik_p} + \frac{i}{2}k_p b^2\rho^2 A_p = \frac{i\omega_p}{c}n_2|A_p|^2 A_p, \tag{7}$$

$$\frac{\partial A_s}{\partial z} + \frac{\nabla_T^2 A_s}{2ik_s} + \frac{i}{2}k_s b^2\rho^2 A_s = \frac{2i\omega_s}{c}n_2|A_p|^2 A_s + \frac{1}{2}g_R|A_p|^2 A_s. \tag{8}$$

Notice that the pump equation is decoupled from the signal's equation and can be solved first to obtain $A_p(\rho, z)$.

For a CW pump in the form of a Gaussian beam, the solution of Eq. (7) was found in 1992 in the form [13],

$$A_p(\rho, z) = \sqrt{\frac{I_p}{f_p}}\exp\left[-\frac{\rho^2}{2w_p^2 f_p} + i\phi_p(\rho, z)\right], \tag{9}$$

where I_p is the peak intensity, w_p is the width of the pump beam at $z = 0$, and the periodic function $f_p(z)$ is defined as

$$f_p(z) = \cos^2(bz) + C_p^2\sin^2(bz). \tag{10}$$

The parameter C_p depends on the width and intensity of the pump beam as

$$C_p = \frac{\sqrt{1 - p}}{bk_p w_p^2}, \quad p = \frac{n_2 I_p}{2n_0}(k_p w_p)^2. \tag{11}$$

The dimensionless parameter p can be written as $p = P_p/P_c$, where $P_p = (\pi w_p^2)I_p$ is the input power of the pump beam and $P_c = 2\pi n_0/(n_2 k_p^2)$ is the critical power at which its collapse occurs owing to self-focusing.

Figure 1 uses the solution in Eq. (9) to show the periodic evolution of a pump beam inside a GRIN fiber for input parameters

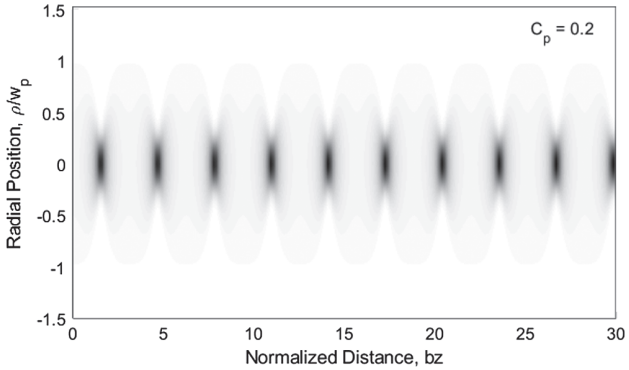

Fig. 1. Periodic focusing and self-imaging of the pump beam inside a GRIN-fiber Raman amplifier. The beam's width is reduced by a factor of 5 for $C_p = 0.2$, and its intensity is enhanced by a factor of 25, at distances such that $bz = (m + \frac{1}{2})\pi$, where m is an integer.

such that $C_p = 0.2$. The pump beam compresses and expands during each period such that it recovers its input shape and width at distances such that $bz = m\pi$, where m is an integer. The maximum compression occurs in the middle of each period where $w/w_p = C_p$, i.e., the parameter C_p dictates the minimum width of the pump beam in each cycle. When the pump's power is considerably below the critical power P_c, resulting in $p \ll 1$ in Eq. (11), the self-focusing effects are relatively minor and can be ignored.

3. AMPLIFICATION OF THE SIGNAL BEAM

In this section, we use the pump solution given in Eq. (9) to solve Eq. (8) satisfied by the signal being amplified. We show that it is possible to obtain an equation governing changes in the width of the signal beam, after making a reasonable approximation. As we saw in Section 2, the nonlinear SPM term has a relatively minor effect on a pump beam whose input power is well below the critical self-focusing level. Assuming that to be the case, the XPM term containing n_2 in Eq. (8) can also be ignored. The pump-induced spatial cleanup effects are not included in our simplified analysis based on the following linear equation for the signal's amplitude:

$$\frac{\partial A_s}{\partial z} + \frac{\nabla_T^2 A_s}{2ik_s} + \frac{i}{2}k_s b^2\rho^2 A_s = \frac{1}{2}g_R|A_p|^2 A_s. \tag{12}$$

We can solve Eq. (12) approximately when the signal at the input end is in the form of a Gaussian beam. We seek its solution in a self-similar form as

$$A_s(\rho, z) = A_0 \exp\left(-\frac{\rho^2}{2w^2} + \frac{ikh}{2}\rho^2 + i\psi\right), \tag{13}$$

where the four parameters (A_0, w, h, and ψ) vary with z. We use this form in Eq. (12) and approximate $|A_p|^2$ from Eq. (9) as

$$|A_p(\rho, z)|^2 \approx \frac{I_p}{f_p}\left(1 - \frac{\rho^2}{w_p^2 f_p}\right). \tag{14}$$

This approximation is justified because the pump beam in practice is wider that the signal beam, and its shape is nearly parabolic over the signal's width. Equating the real and imaginary parts on the two sides of Eq. (12) for terms containing different powers of ρ, we obtain the following first-order differential equations for the four parameters:

$$\frac{dA_0}{dz} = \frac{g_R I_p}{2f_p}A_0 - hA_0, \tag{15}$$

$$\frac{dw}{dz} = hw - \frac{g_R I_p}{2w_p^2 f_p^2}w^3, \tag{16}$$

$$\frac{dh}{dz} = \frac{1}{k_s^2 w^4} - h^2 - b^2, \tag{17}$$

$$\frac{d\psi}{dz} = -\frac{1}{k_s w^2}. \tag{18}$$

The presence of the Raman gain modifies equations for both A_0 and w. The amplitude in Eq. (15) is expected to increase with z because of the Raman gain. However, as seen from Eq. (16), the Raman gain also affects the width of the signal beam.

Consider first the case of a relatively wide pump beam for which the last term in Eq. (16) can be neglected. Using $hw = dw/dz$ in Eq. (15), we can write this equation as

$$\frac{d}{dz}(w^2 A_0^2) = \frac{g_R I_p}{f_p(z)}(w^2 A_0^2). \tag{19}$$

Recalling that the signal's power at any distance z is given by

$$P_s(z) = \int_0^{2\pi} d\phi \int_0^{\infty} |A_s(\rho, z)|^2 \rho d\rho = (\pi w^2) A_0^2, \tag{20}$$

we can write Eq. (19) in the form

$$\frac{dP_s}{dz} = \frac{g_R I_p}{f_p(z)} P_s. \tag{21}$$

Integrating this equation, the signal's power is found to increase inside the amplifier as

$$P_s(z) = P_s(0)\exp\left(g_R I_p \int_0^z \frac{dz'}{f_p(z')}\right). \tag{22}$$

Because of the GRIN-induced self-imaging of the pump beam, $P(z)$ oscillates in a periodic fashion, as the signal is amplified through the Raman gain. It is important to consider the length scale of such oscillations. Whereas amplification occurs over a length scale of meters, the self-imaging period for typical GRIN fibers is ~1 mm. For this reason, one can average the integral in Eq. (22) over one self-imaging period. Using $I_p = P_p/(\pi w_p^2)$, where P_p is the input pump power, we obtain

$$P_s(z) = P_s(0)\exp(g_{\text{eff}} z), \quad g_{\text{eff}} = \frac{g_R P_p}{\pi w_p^2 C_p}. \tag{23}$$

This result shows that the signal's power grows exponentially inside a GRIN Raman amplifier with an effective gain coefficient that depends on the pump beam's parameters.

Our main interest in this work is in finding how the width of the signal beam changes during its amplification inside the GRIN Raman amplifier. Calculating the second derivative of w from Eq. (16) and using Eq. (17), we obtain the following equation for the width $w(z)$:

$$\frac{d^2 w}{dz^2} + b^2 w = \frac{1}{k_s^2 w^3} - \frac{g_R I_p}{2w_p^2}\frac{d}{dz}\left(\frac{w^3}{f_p^2}\right). \tag{24}$$

Thus, the problem has been reduced to solving a single second-order differential equation for the beam's width. Physically, the two terms on the right side of this equation represent, respectively, the effects of diffraction and of the Raman gain. For pump beams much wider than the signal, the Raman term in Eq. (24) becomes negligible. The width equation in this specific case can be solved analytically to obtain [12,13]

$$w(z) = w_s\sqrt{f_s(z)}, \quad f_s(z) = \cos^2(bz) + C_s^2\sin^2(bz), \tag{25}$$

where $C_s = (bk_s w_s^2)^{-1}$ and w_s is the initial width of the signal beam at $z = 0$. Similar to the pump beam, the signal beam also

evolves in a periodic fashion dictated by the self-imaging phenomenon. The self-imaging period, defined as $L_p = 2\pi/b$, is only about 1 mm for typical GRIN fibers. Notice that L_p is the same for both the pump and signal beams but the compression factors, C_p and C_s, become different for them.

4. RAMAN-INDUCED NARROWING OF THE SIGNAL BEAM

In this section, we solve Eq. (24) approximately to study how the width of the signal beam is affected by the Raman gain. For this purpose, it is useful to normalize Eq. (24) using $s = w/w_s$ and $\xi = bz$, where w_s is the initial width of the signal beam at $z = 0$. The normalized form of the width equation is

$$\frac{d^2 s}{d\xi^2} + s = \frac{C_s^2}{s^3} - \mu \frac{d}{d\xi}\left(\frac{s^3}{f_p^2}\right), \tag{26}$$

where the two dimensionless parameter are defined as

$$\mu = \frac{g_R I_p w_s^2}{2b w_p^2}, \quad C_s = \frac{w_g^2}{w_s^2}, \tag{27}$$

with $w_g^2 = 1/(bk_s)$. Physically, w_g represents the width of the fundamental mode of the GRIN fiber at the signal's frequency. Its value is about 5 μm for GRIN fibers. The last term in Eq. (26), representing the effects of the Raman gain, depends on both the intensity and the width of the pump beam inside the GRIN medium.

The second-order nonlinear differential equation in Eq. (26) can be solved numerically with a suitable technique such as the Runge–Kutta method. Figure 2 shows the results for $\mu = 0.01$ (top) or $\mu = 0.02$ (bottom) using $C_s = 0.2$ and $C_p = 0.1$. As expected, the signal's width oscillates because of self-imaging. The new feature in Fig. 2 is that the amplitude of oscillations decreases the width distance, and the damping rate of oscillations increases with μ.

The important question is what values of μ are realistic for a GRIN Raman amplifier. Using $I_p = P_p/(\pi w_p^2)$, where P_p is the input pump power, we can write the parameter μ in the form

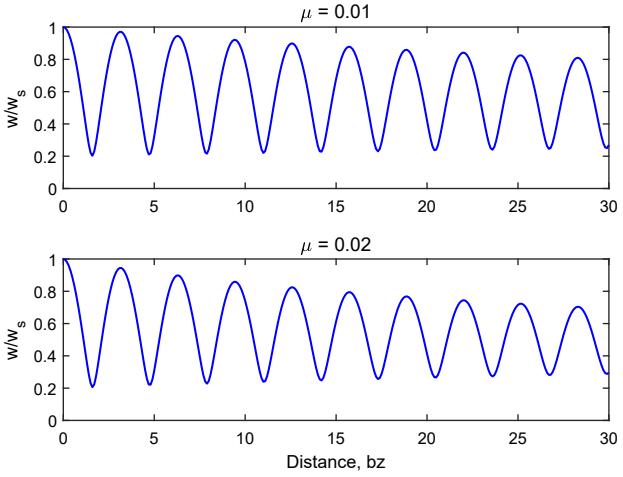

Fig. 2. Oscillations in the width of the signal beam for two values of the parameter μ. The amplitude of oscillations does not change when $\mu = 0$.

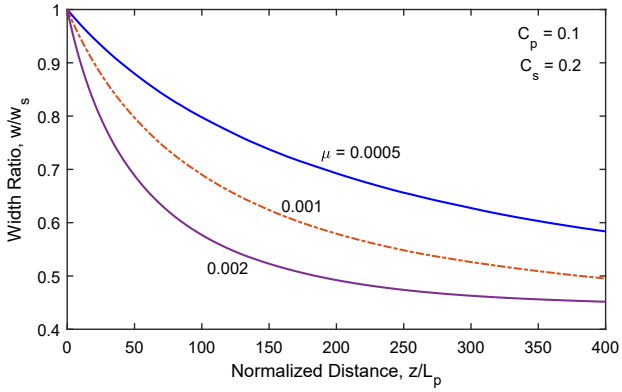

Fig. 3. Predicted decrease in the width of the signal beam as a function of z/L_p for three values of the parameter μ.

$$\mu = \frac{g_R P_p L_p w_s^2}{4\pi^2 w_p^4}. \tag{28}$$

This expression shows that the width of the pump beam play a crucial role because μ scales inversely with it as $1/w_p^4$. When the pump beam is much wider than the signal beam, μ may become so small ($\mu < 10^{-6}$) that little narrowing of the amplified signal can occur over the length of the Raman amplifier. Even when the two beams have comparable widths at the input end, the value of μ is $\sim 10^{-4}$, indicating that significant narrowing of the signal beam is expected to occur after thousands of oscillations in Fig. 2.

As an example, Fig. 3 shows the numerically predicted decrease in the width of a signal beam over 400 self-imaging periods for three values of μ using $C_p = 0.1$ and $C_s = 0.2$. The maximum value of the width at the end of each self-imaging period was plotted to show the envelope without any oscillations. Relatively large values of μ were used to reduce the computing time, but the same qualitative behavior is expected for smaller values of μ. In all cases, the width decreases in an exponential fashion. For $\mu = 0.002$, it appears to have reached its final value that is only 45% of the input width at a distance of $400 L_p$. For smaller values of μ, a longer distance is needed to reach the steady-state value of the width.

As numerical solutions do not provide much physical insight, we solve Eq. (26) approximately. Its solution is known when $\mu = 0$ and can be written from Eq. (25) as

$$s(\xi) = \sqrt{f_s(\xi)}, \quad f_s(\xi) = 1 - (1 - C_s^2)\sin^2\xi. \tag{29}$$

The Raman term affects this solution over a much longer length scale compared to L_p. However, this term depends on $f_p^2(\xi)$ and varies rapidly with ξ. To include its impact approximately, we replace $f_p^2(\xi)$ with its average value and write Eq. (26) as

$$\frac{d^2 s}{d\xi^2} + \frac{3\mu s^2}{\langle f_p^2\rangle}\frac{ds}{d\xi} + s = \frac{C_s^2}{s^3}, \tag{30}$$

where the angle brackets denote the average over one self-imaging period. The average of $f_p^2(\xi)$ over one self-imaging period can be calculated from Eq. (10) and is found to be

$$\langle f_p^2\rangle = C_p^2 + \frac{3}{8}(1 - C_p^2)^2. \tag{31}$$

As a further simplification, we replace s^2 with $\langle f_s \rangle$ in the second term in Eq. (30). This is justified as long as L_p is a small fraction of the amplifier's length (>10 m in practice). If we also neglect the small term containing C_s^2, we obtain a linear equation similar to that of a damped harmonic oscillator,

$$\frac{d^2 s}{d\xi^2} + 2\gamma_d \frac{ds}{d\xi} + s = 0, \tag{32}$$

where the damping rate is governed by the parameter γ_d defined as

$$\gamma_d = \frac{3\mu \langle f_s \rangle}{2\langle f_p^2 \rangle}. \tag{33}$$

The solution of Eq. (32) for an initially collimated beam is $s(\xi) = \cos\xi \exp(-\gamma_d \xi)$. We can include the diffraction effects, governed by the last term in Eq. (30), by writing its approximate solution as $s(\xi) = \sqrt{f_s} e^{-\gamma_d \xi}$. In terms of the original variables, the solution takes the form

$$w(z) = w_s \sqrt{f_s(z)} \exp(-\gamma_d b z). \tag{34}$$

This analytic solution shows that the width of the signal beam oscillates inside a GRIN Raman amplifier with a period ~1 mm, but the amplitude of oscillations decreases on a length scale L_d governed by the decay rate γ_d. This length scale depends on the input parameters as

$$L_d = \frac{1}{b\gamma_d} = \frac{8\pi w_p^4 \langle f_p^2 \rangle}{3 g_R P_p w_s^2} (1 + C_s^2)^{-1}, \tag{35}$$

where we used $\langle f_s \rangle = (1 + C_s^2)/2$.

In practice, the parameter C_p for the pump beam is much smaller than 1. Neglecting C_p^2 in Eq. (31), we can write Eq. (35) in terms of the known input parameters as

$$L_d = \frac{\pi w_p^4 (1 + C_s^2)^{-1}}{g_R P_p w_s^2}. \tag{36}$$

Noting that L_d scales as w_p^4, we conclude that the width of the pump beam plays a crucial role. Specifically, for wide pump beams, L_d may be much longer than the length of the Raman amplifier, resulting in negligible narrowing of the signal beam.

5. DISCUSSION AND CONCLUSIONS

The length L_d depends on the input power of the pump beam as well as on the initial widths of the pump and signal beams. We can estimate its value for silica-based GRIN fibers using $g_R = 1 \times 10^{-13}$ m/W for the Raman gain at wavelengths near 1 μm [2]. At a pump power of 1 kW, the peak intensity is close to 1 TW/m^2. If we use $w_p/w_s = 2$, L_d is estimated to be about 20 m. This value is much larger compared to the self-imaging period (about 1 mm) in typical GRIN fibers. As the fiber's length in a Raman amplifier typically exceeds 20 m, considerable narrowing of the signal beam can occur over its length. If the signal beam's width is reduced to near 5 μm before the output end of the GRIN fiber, it will nearly match the width of the fiber's fundamental mode. As a result, most of the signal's power at the output end will be in the fundamental mode of the GRIN fiber. This conclusion agrees with a detailed mode-based numerical model [11].

To judge the usefulness of Eq. (36) in practice, we focus on two recent experiments on Raman amplifiers. A 100-m-long double-clad GRIN fiber was used in a 2018 experiment [4]. Its core, with a diameter of 62.5 μm, was encased in the inner cladding whose diameter was 125 μm, but the outer-cladding diameter exceeded 300 μm. The GRIN fiber was cladding-pumped at 1018 nm using a relatively wide pump beam. The output power of the amplified 1060-nm signal was 654 W when the pump power was 766 W, resulting in a conversion efficiency of 85%. The quality of the output beam was judged by measuring its M^2 factor [14]. The measured value was 4.2, indicating a quality far from that of a Gaussian beam. The estimated value of L_d for this experiment exceeds 200 m because of the use of a much wider pump beam compared to that of the signal.

In a 2020 experiment [5], only a 20-m-long piece of GRIN fiber was employed to suppress the onset of the second-order Stokes inside the amplifier. The fiber has a single cladding of 125 μm diameter, and its core had a diameter of 62.5 μm. The pump beam was relatively narrow because it was launched using fibers of 20-μm core diameters. The 1130-nm signal beam could be amplified up to a power level of 2 kW, with a conversion efficiency of 80%. The measured value of M^2 was close to 2.8 at the high pump-power level used in this experiment. This improvement in beam's quality is expected from Eq. (36) because L_d is reduced to near 30 m in this experiment, resulting in a narrower signal beam, with a large fraction of its power in the fundamental mode of the GRIN fiber.

It is important to emphasize that the results of this paper should not be used for a quantitative comparison with the experiments in view of the approximations and simplifications made in obtaining them. The analysis ignores the polarization effects and assumes that both pump and signal are coherent, CW, Gaussian-shaped beams. It does not make use of the modal description and cannot include random mode coupling that occurs in long fibers. The analysis also neglects the pump-induced XPM effects, assuming that the pump's power is considerably below a critical self-focusing threshold. These approximations are reasonable for single-clad GRIN fibers, pumped longitudinally by launching an intense Gaussian beam at power levels below the self-focusing threshold [5]. However, their use becomes questionable for cladding-pumped Raman amplifiers employing much wider pump beams with a nearly flat intensity profile.

In conclusion, a simple semi-analytic model is presented that allows us to study spatial beam narrowing in GRIN-fiber Raman amplifiers, pumped such that the optical gain is spatially nonuniform in the radial direction. An analytic expression for the width of the signal beam is obtained after making some reasonable approximations. It shows that the signal beam narrows down on a length scale ~1 m, as it is amplified inside the GRIN fiber, while exhibiting periodic self-imaging on a length scale ~1 mm. The predicted beam narrowing has its origin in the pump-induced radial dependence of the optical gain. The main advantage of our simplified approach is that it provides an analytic expression for the damping rate of oscillations, which shows clearly the role played by various physical parameters. For example, the width of the pump beam is found to play a crucial

role. Little improvement in spatial quality of the amplified beam is likely to occur when the Raman amplifier is cladding-pumped using wide pump beams. In contrast, considerable improvement in the beam's quality can occur when the pump and signal beams have comparable sizes and are launched together into the GRIN fiber.

Funding. National Science Foundation (ECCS-1933328).

Disclosures. The author declares no conflicts of interest.

Data availability. Data underlying the results presented in this paper are not publicly available at this time but may be obtained from the author upon reasonable request.

REFERENCES

1. M. N. Islam, *Raman Amplifiers for Telecommunications* (Springer, 2003).
2. G. P. Agrawal, *Nonlinear Fiber Optics*, 6th ed. (Academic, 2019).
3. L. Sirleto and M. A. Ferrara, "Fiber amplifiers and fiber lasers based on stimulated Raman scattering: a review," Micromachines **11**, 247 (2020).
4. Y. Chen, J. Leng, H. Xiao, T. Yao, and P. Zhou, "High-efficiency all-fiber Raman fiber amplifier with record output power," Laser Phys. Lett. **15**, 085104 (2018).
5. Y. Chen, T. Yao, H. Xiao, J. Leng, and P. Zhou, "Greater than 2 kW all-passive fiber Raman amplifier with good beam quality," High Power Laser Sci. Eng. **8**, e33 (2020).
6. Y. Chen, T. Yao, H. Xiao, J. Leng, and P. Zhou, "3-kW passive-gain-enabled metalized Raman fiber amplifier with brightness enhancement," J. Lightwave Technol. **39**, 1785–1790 (2021).
7. C. Fan, H. Xiao, T. Yao, J. Xu, Y. Chen, J. Leng, and P. Zhou, "Kilowatt level Raman amplifier based on 100 μm core diameter multimode GRIN fiber with $M^2 = 1.6$," Opt. Lett. **46**, 3432–3435 (2021).
8. N. B. Terry, T. G. Alley, and T. H. Russell, "An explanation of SRS beam cleanup in graded-index fibers and the absence of SRS beam cleanup in step-index fibers," Opt. Express **15**, 17509–17519 (2007).
9. N. B. Terry, K. Engel, T. G. Alley, T. H. Russell, and W. B. Roh, "Beam quality of the Stokes output of continuous-wave Raman fiber amplifiers using multimode fiber," J. Opt. Soc. Am. B **25**, 1430–1436 (2008).
10. G. P. Agrawal, "Self-imaging in multimode graded-index fibers and its impact on the nonlinear phenomena," Opt. Fiber Technol. **50**, 309–316 (2019).
11. O. S. Sidelnikov, E. V. Podivilov, M. P. Fedoruk, A. G. Kuznetsov, S. Wabnitz, and S. A. Babin, "Mechanism of brightness enhancement in multimode LD-pumped graded-index fiber Raman lasers: numerical modeling," Opt. Express **30**, 8212–8221 (2022).
12. G. P. Agrawal, *Physics and Engineering of Graded-Index Media* (Cambridge University, 2023).
13. M. Karlsson, D. Anderson, and M. Desaix, "Dynamics of self-focusing and self-phase modulation in a parabolic index optical fiber," Opt. Lett. **17**, 22–24 (1992).
14. A. E. Siegman, "New developments in laser resonators," Proc. SPIE **1224**, 2–14 (1990).